ELSEVIER

On the performance of radiant barriers in combination with different attic insulation levels

Mario A. Medina Ph.D., P.E. [*]

Architectural Engineering Department, The University of Kansas, Lawrence, KS 66045-2222, USA

Abstract

Experiments and computer simulations were conducted to evaluate the performance of radiant barriers under three different insulation levels in residential applications. The experiments were conducted in central Texas, USA using side-by-side comparisons in which two houses, with identical floor plans and thermal profiles, were used. The houses were instrumented, calibrated, and their heat transfer rates across the ceilings were measured and recorded. A heat and mass transfer model was used to run the computer simulations. The results suggest that the reductions in heat transfer (on a percentage basis) produced by the radiant barriers decrease as the attic insulation resistance increases. On average, the experimental summer heat flow reductions produced by the radiant barriers in combination with attic insulation resistance levels of 1.94, 3.35, and 5.28 m^2 K/W ($R=11$, 19, and 30) were 42, 34, and 25%, respectively. The simulations, driven by typical meteorological year (TMY) data, produced yearly heat flow reductions of approximately 44, 28, and 23% for the same insulation levels, respectively. © 2000 Elsevier Science S.A. All rights reserved.

Keywords: Radiant barriers; Building heat and mass transfer; Heat balance modeling

1. Introduction

A significant amount of the cooling load in residential buildings is the result of heat transfer across the ceiling from the attic space. The ceiling heat flow originates with the incident solar radiation that is absorbed by the roof. The amount of heat that is not re-radiated or convected from the roof is conducted across the attic decking material. Of the heat that arrives at the opposite surface of the deck, part is convected to the attic air and the rest is radiated to the ceiling frame, the lateral end-gables, and other roof sections. The net heat that is absorbed by the ceiling frame during the radiation exchange is both convected to the attic air and transported in the direction of decreasing temperature into the conditioned space where it becomes part of the cooling load. In general, except for the solar energy that is absorbed by the roofing materials, heat transfer processes in the heating season are similar to those described above but in the reverse direction.

The most appreciable deviation from base load utility costs in residences occurs in the summer months as a consequence of increased air-conditioning equipment run-time. For this reason, and because one of the major components of the cooling load from the ceiling is infrared radiation from the hot attic deck, radiant barriers are successfully being used to obstruct the transfer of heat from the attic into the conditioned space.

Radiant barriers are sheets of aluminium foil that are normally adhered to a fiberglass mesh to keep them from tearing. In new constructions, the aluminized surface is glued to the underside of the decking material. In retrofit applications, radiant barriers are installed in several arrangements, two of which are the most commonly used installations. In one, the barrier is installed horizontally over the attic frame (horizontal radiant barrier, HRB). This configuration is shown in Fig. 1. In the other configuration, the barrier is attached to the rafters that support the deck (truss radiant barrier, TRB). This is shown in Fig. 2. Concerns related to the adverse effect of dust and other particulate accumulation in HRB installations, together with the issue of reserving attic space for storage purposes, have made the use of this configuration unsuitable for residential use. Thus, the results presented in this paper apply mainly to the TRB installation.

A parameter that affects the performance of the radiant barriers is the level of attic insulation that is present in the

[*] Tel.: +1-785-864-3434; fax: +1-785-864-5099.
E-mail address: mmedina@ukans.edu (M.A. Medina)

Nomenclature

A, A	matrix of coefficients, surface area
B	vector of known coefficients
CR	common ratio (unitless)
h_i, h_o	heat transfer coefficient (W/m^2 K, Btu/h ft^2 °R)
h_{ri}, h_{ro}	linearized radiation heat transfer coefficients (W/m^2 K, Btu/h ft^2 °R)
HRB	horizontal radiant barrier
L	equivalent width (m, ft)
q''	heat flux (W/m^2, Btu/h ft^2)
T	temperature (K, °R)
T_r	reference temperature (K, °R)
TRB	truss radiant barrier
T_{si}	inside surface temperature (K, °R)
T_{so}	outside surface temperature (K, °R)
X, Y, Z	response factors (W/m^2 K, Btu/h ft^2 °R)

Greek Symbols

α	solar absorptivity
ε	thermal emissivity
η	coordinate axis of air flow

Subscripts

$0, 1, 2, \ldots$	time denoting index (response factors)
amb	ambient conditions
i	denotes surface, index, indoor conditions
j	denotes time, index
k	denotes surface
$n\Delta$	time step
o	outdoor
RB	radiant barrier
sol	solar
surr	surroundings

Index

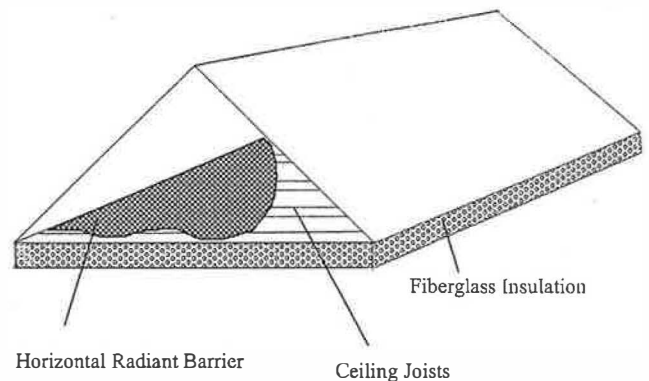| N	number of surfaces
S	number of time steps

Fig. 1. Horizontal radiant barrier configuration.

and produced by the combination of soffit louvers and gable vents.

The following conclusions were drawn from Fig. 3: (1) the relative ceiling heat flow reduction, on a percentage basis, decreases as the insulation level increases; (2) most of the existing literature reports results of experiments that were carried out using insulation with a resistance value of approximately 3.35 m^2 K/W (R=19); and (3) reported results from experiments that used the same level of insulation resistance differed substantially from one another. This could be because of different weather patterns and/or because of the quality of the data and sensors used. The research presented in this paper adds to the existing literature by providing results of experiments that were carried out using three insulation levels with resistances of 1.94, 3.35, and 5.28 m^2 K/W (R=11, 19, and 30). In addition, monthly simulations of ceiling heat flow reductions produced by radiant barriers in combination with the three insulation resistance levels are presented.

The percent reduction in heat transfer was estimated by

Percentage ceiling heat flow reduction

$$= \frac{\int_{\text{test period}} q''_{\text{no RB}} \, dt - \int_{\text{test period}} q''_{\text{RB}} \, dt}{\int_{\text{test period}} q''_{\text{no RB}} \, dt} \times 100 \qquad (1)$$

2. Physical model and computer code

A physical model of the thermal and mass processes experienced by attic structures was developed using a heat balance methodology [5,6]. The model was based on the first law of thermodynamics and it allowed instantaneous sensible and latent cooling and heating loads to be calculated based on energy balance equations written for each enclosing surface and for attic air layers. These equations were written in terms of unknown temperatures based on heat transfer processes and using previous temperatures and heat fluxes as well as physical descriptions of the attic components.
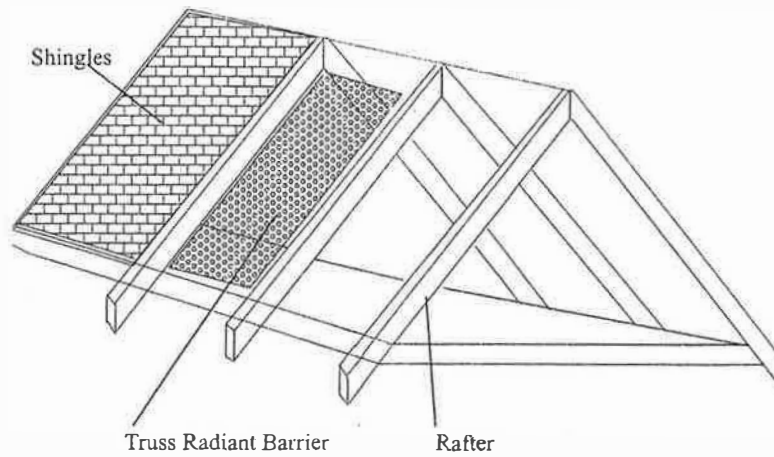
building. This is shown in Fig. 3. This graph was constructed from published experimental data [1–4]. For the present study, the size of the data set found in the open literature was reduced by selecting only those studies that met the following criteria: (1) attics of similar construction and geometry; (2) attics with similar ventilation arrangement; (3) attics exposed to outdoor conditions; and (4) reported results that included both daytime and nighttime hours. Under these criteria, the data selected came from experiments conducted in houses with pitched roofs made up of asphalt shingles and plywood decking. In most cases, attic ventilation was natural

Fig. 2. Truss radiant barrier configuration.

The processes were coupled by a series of linear equations of the form

$$\sum_{j=0,i=1}^{N,S} Y_{i,j}(T_{si_{i,n\Delta-j}} - T_r) - \sum_{j=0,i=1}^{N,S} X_{i,j}(T_{so_{i,n\Delta-j}} - T_r)$$
$$+ CR_i q''_{o(i,n\Delta-j)} + h_{o_i}(T_{amb} - T_{so_i,n\Delta})$$
$$+ \sum_{k=1,i=1}^{S,S} h_{ro_i}(T_{sky/surr} - T_{so_i,n\Delta}) + \alpha q''_{sol,i} = 0 \quad (2)$$

for exterior surfaces,

$$\sum_{j=0,i=1}^{N,S} Z_{i,j}(T_{si_{i,n\Delta-j}} - T_r) - \sum_{j=0,i=1}^{N,S} Y_{i,j}(T_{so_{i,n\Delta-j}} - T_r)$$
$$+ CR_i q''_{i(i,n\Delta-j)} + h_{j_i}(T_{si_{i,n\Delta}} - T_{attic\,air,n\Delta})$$
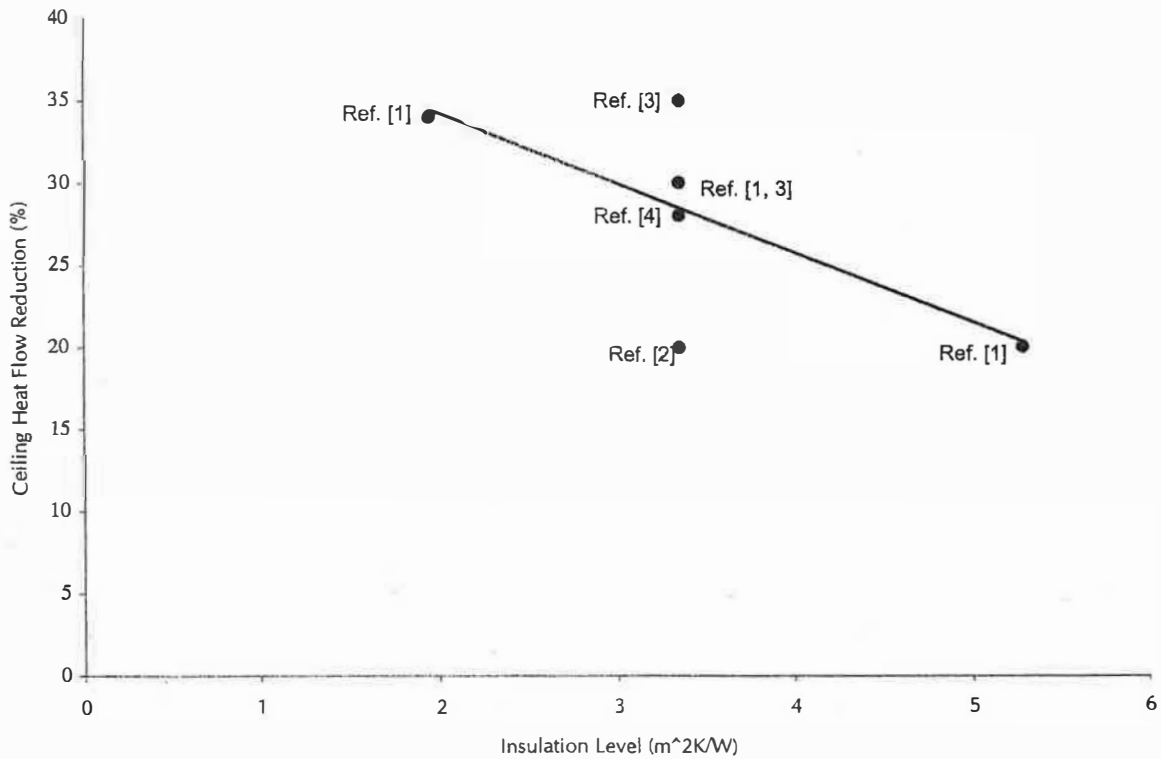$$+ \sum_{k=1,i=1}^{S,S} h_{ri_{i,k}}(T_{si_{i,n\Delta}} - T_{si_{k,n\Delta}}) + q''_{latent,i} = 0 \quad (3)$$

Fig. 3. Heat flow reduction as a function of attic insulation level (literature).

for interior surfaces, and

$$\dot{m}C_{p}\frac{\mathrm{d}T}{\mathrm{d}\eta} = \sum_{i=1}^{N} L_{i}h_{i_{i}}(T_{\mathrm{si}_{i,n\Delta}} - T_{\mathrm{attic\ air},n\Delta}) \tag{4}$$

for attic air. In Eqs. (2) and (3) the X, Y, Z, and CR represent conduction transfer functions and common ratio; T_{si}, T_{so}, and T_{r} are inside surface, outside surface, and reference temperatures (K, °R), respectively; h_{i} and h_{o} are convection heat transfer coefficient for indoor and outdoor surfaces (W/ m^{2} K, Btu/h ft^{2} °R), respectively; and h_{ri} and h_{ro} represent linearized radiation coefficients for the indoor and outdoor (W/m^{2} K, Btu/h ft^{2} °R), respectively. In Eq. (4), η refers to the coordinate along which the attic air flowed.

The convection coefficients were calculated using published correlation for forced and natural flows [7,8]. Radiation was handled via radiation enclosure theory [9]. Solar radiation on outer surfaces was calculated by separating the total hemispherical solar irradiation into its direct and diffuse components. The direct components on each surface were calculated as described in [10]. Latent effects were incorporated via a condensation and evaporation model [11,12].

The simulations were produced by implementing the model with a computer program that used an iterative process to predict temperatures and heat fluxes using linear algebra principles. The development of the computer program included information on the attic construction type (conduction transfer functions), dimensions, radiation constants (outer surface absorptivities, outer and inner surface emissivities), moisture transport parameters (percent surface area covered with wood, permeability of each attic component and wood moisture content), and location data (longitude, latitude, and time zone). View factors were calculated and stored for later use. Hourly weather data were input one time step ($n\Delta$ of 1 h) at a time. These data included day, hour of the day, outdoor air temperature, solar radiation on a horizontal surface, wind speed, relative humidity or dew point temperature, and cloud clover data. All of these information was set up in a matrix of coefficients and a vector of known parameters, matrix A and vector B, respectively. Temperatures were then calculated by

$$AT = B \tag{5}$$

The solution procedure required that updated values of A and B be calculated and then used to solve for temperatures using Eq. (5). The A matrix contained X, Y, and Z conduction transfer functions, convection and radiation coefficients, and attic air stratification information. The B vector included historical values of all surface temperatures, previous values of heat fluxes at each surface, outdoor air temperature, indoor air temperature, solar loads, sky and surrounding air temperatures, convection and radiation coefficients, X, Y, and Z conduction transfer functions, and common ratio, CR. An iterative process, in which new values of temperatures were calculated and compared to pre-set tolerances, was carried out. If the new values computed in the last iteration

minus the values of the next to the last iteration differed by more than the tolerance, the process started over. The newly calculated values were used to re-estimate all coefficients until convergence was achieved. After convergence, the heat fluxes were calculated. The final set of temperatures and the previous heat flux were stored for later use to account for transient effects. The outputs of the program were hourly surface temperatures, attic air temperatures, and heat fluxes. The performance evaluation of radiant barriers in this study was done based on ceiling heat transfer reductions. The comparisons between control and retrofit houses as well as between model predictions and the data are, therefore, presented in terms of ceiling heat fluxes.

3. Model verification

The model was verified against experimental data. The experimental data were obtained from radiant barrier studies conducted in central Texas, USA in which two identical single-room test houses with identical thermal profiles were used [4]. The identical thermal profiles of the houses were verified via null testing.

Fig. 4 depicts a comparison of model prediction to experimental data. These data were from summer experiments in which the days shown were from July. During this period, the attic airflow rate in the test houses was 5.1 l/s/m^{2} (1.0 CFM/ft^{2}). It was decided to use forced attic ventilation instead of natural attic ventilation in order to have a quantitative measure of the airflow to both attics and to eliminate the possibility of the attics experiencing different airflow rates. Previous results [4] had showed that a critical attic ventilation flowrate of 1.3 l/s/m^{2} (0.25 CFM/ft^{2}) existed after which the percentage reduction in ceiling heat fluxes produced by the radiant barriers did not change with increasing attic airflow rate. A rate of 5.1 l/s/m^{2} (1 CFM/ft^{2}) was selected because of the reduction in reading error that resulted when high airflow rates were used. The attic insulation had a nominal resistance value of 3.35 m^{2} K/W (R=19).

As depicted in Fig. 4, the computer predictions were in good agreement with the data during both peak and off-peak times. The cumulative difference between data and predictions was <2%. The curves in Fig. 4 include 48 h of data arranged in a 24 h span, thus, creating what appears as two distinct curves. (The same is true for Fig. 5). The ceiling heat fluxes (data) were measured using heat flow sensors. Eighty percent of the sensors were attached to the underside of the ceiling wallboard and the others rested on top of the ceiling wallboard on the attic side. Twenty percent of the sensors measured the conduction across ceiling joists. All the reported ceiling heat fluxes are weighted averages representative of the areas covered by the sensors. The anomalous data of 12 noon is the result of an abrupt off–on process on the datalogger that was needed to download data into a microcomputer.
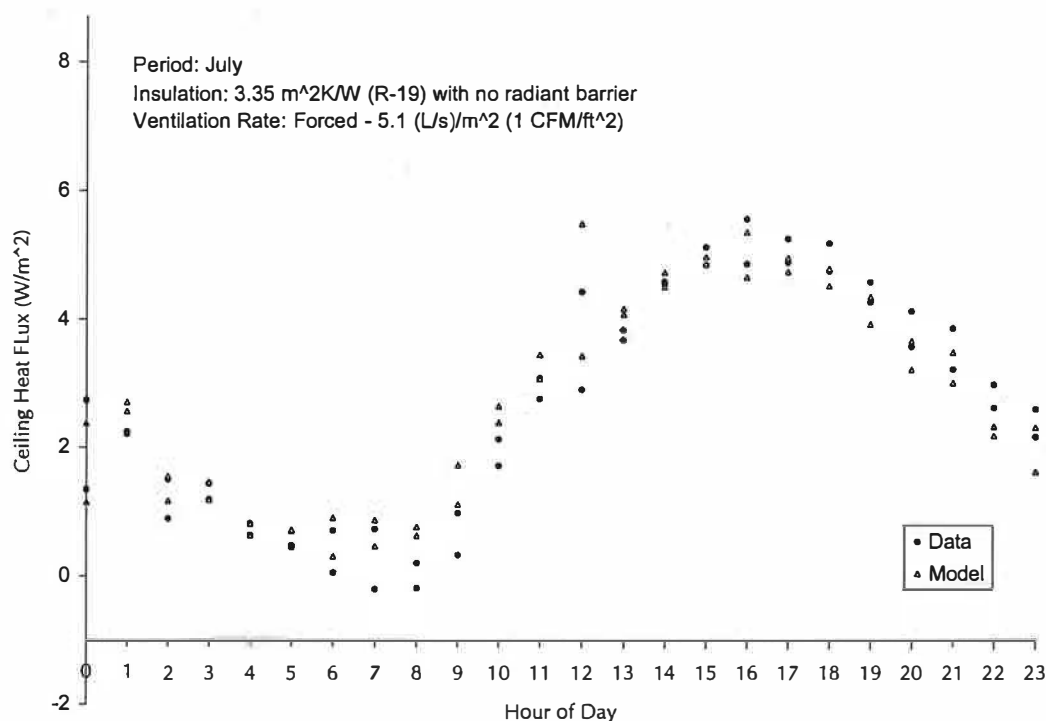
Fig. 4. Measured and predicted heat fluxes (no-RB-case, insulation resistance: 3.35 m^2 K/W, *R*-19).

Several modifications were made to the program to run the retrofit case simulations. These included the calculation of convection and radiation coefficients in the new air space that was formed between the radiant barrier and the attic deck, the radiation interaction between the radiant barrier and the attic deck, and the addition of a second moisture balance in the newly formed air space. The rafters were assumed to be re-radiating surfaces.

Fig. 5 shows a retrofit case that consisted of installing a truss radiant barrier with low emissivity on both sides in
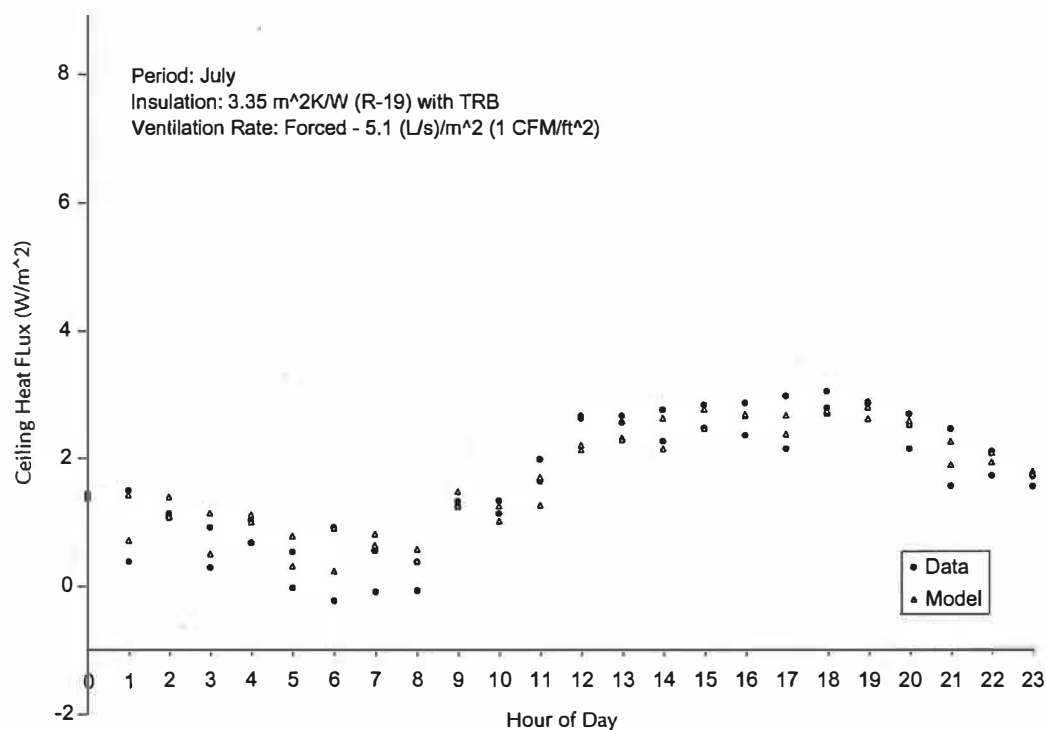

Fig. 5. Measured and predicted ceiling heat fluxes (TRB case, insulation resistance: 3.35 m^2 K/W, *R*-19).

one of the houses. The data also correspond to tests carried out during the month of July. The attic ventilation rate was 5.1 l/s/m^2 (1 CFM/ft^2) and the resistance value of the fiberglass insulation had a nominal value of 3.35 m^2 K/W (R=19). The percent ceiling heat flow reductions produced by the radiant barrier between experiments of Figs. 4 and 5 were on the order of 34%.

The emissivity of the radiant barrier used in the simulations was estimated using

$$\varepsilon_{RB} = \varepsilon_{\text{aluminium}}\%A_{\text{aluminium}} + \varepsilon_{\text{perforation}}\%A_{\text{perforation}}$$
$$= 0.05\,(0.95) + 0.90\,(0.05) = 0.0925 \tag{6}$$

Ventilation in the TRB case was handled similarly to the base case, except that ventilation in the extra air space between the radiant barrier and the attic deck was accounted for by assuming that the airflow was induced by both thermal effects and by pressure effects. The model predictions of Fig. 5 were also within 2% of the measured data.

4. Attic insulation studies

Residential attics are typically insulated with lightweight fibrous insulation, such as fiberglass batts, rock wool, slag wool, or blown insulation. In practice, the exact resistance value of the insulation is unknown. Even when the insulation is in batt form and its nominal value is provided; the actual resistance value depends on how it is installed.

For this study, one summer was dedicated to testing the performance of TRBs in combination with different attic insulation levels. Two houses, located in central Texas, USA, with identical floor plans and thermal profiles were used. The climate in this part of the country is subtropical with hot and humid summers and short and mild winters. The thermal performances of the houses prior to any retrofit were verified via null tests. Total pre-retrofit ceiling heat load difference between the houses was <1% [4]. Both the radiant barrier and the fiberglass were new at the time of installation. The resistance values of the fiberglass insulation were 1.94, 3.35, and 5.28 m^2 K/W (R=11, 19, and 30). In all tests the attic ventilation rate was 5.1 l/s/m^2 (1 CFM/ft^2).

Results of both the base case and retrofit case are presented for each insulation value as well as with their respective model predictions. Fig. 6 shows the performance of a truss radiant barrier in combination with insulation with resistance of 1.94 m^2 K/W (R=11). The experiments suggested heat flow reductions, produced by the radiant barriers, in the range of 42%. On average, the model predictions of the no-RB-case and retrofit case were within 2% of experimental readings. Fig. 7 shows the heat flux when an insulation resistance of 5.28 m^2 K/W (R=30) was used. The experiments suggested reductions in ceiling heat flow, produced by the radiant barriers, in the range of approximately 25%. As far as modeling, while the no-RB-case in Fig. 7 agreed well with the data, the retrofit case was as much as 15% off. The reason for the discrepancy could be the uncertainty over the true thickness of the insulation in the
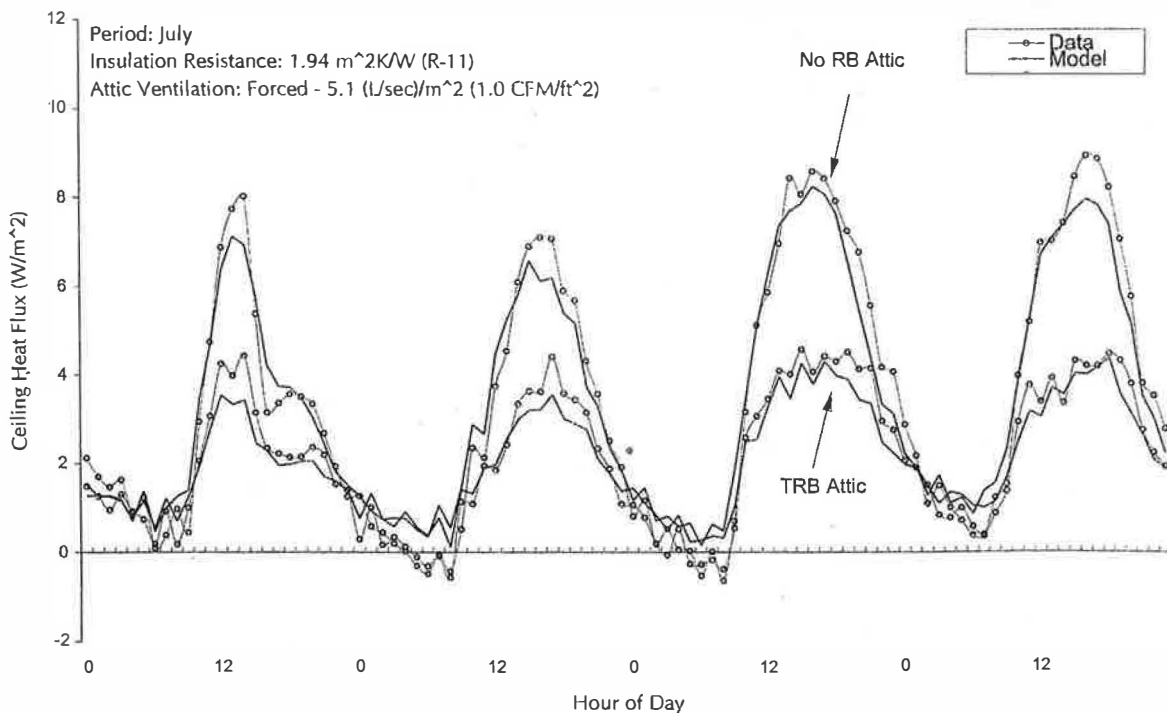

Fig. 6. Ceiling heat fluxes (TRB case, insulation resistance: 1.94 m^2 K/W, R-11; with attic airflow rate: 5.1 l/s/m^2, 1.0 CFM/ft^2).
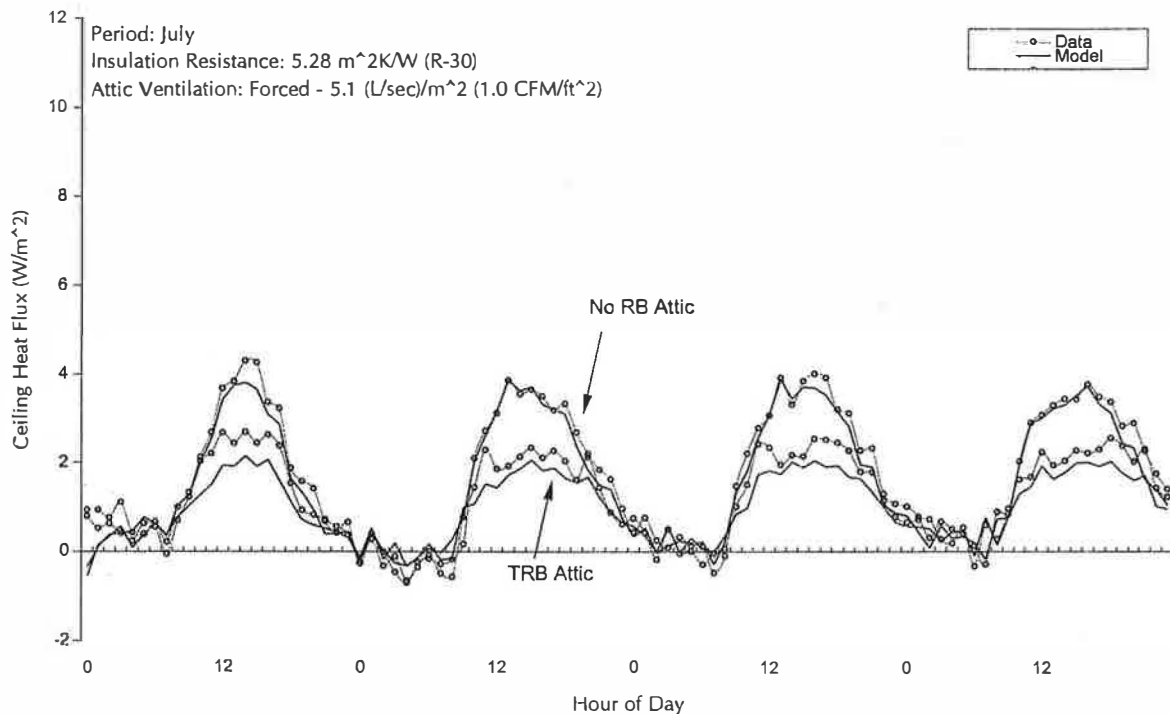
Fig. 7. Ceiling heat fluxes (TRB case, insulation resistance: 5.28 m² K/W, R-30; with attic airflow rate: 5.1 l/s/m², 1.0 CFM/ft²).

retrofit attic. The resistance value of 5.28 m² K/W ($R=30$) was obtained by placing 8.9 cm (3.5 in.) of extra insulation batt on top of a batt of nominal thickness of 15.2 cm (6 in.), thus, making the entire frame of a nominal thickness of 24.1 cm (9.5 in.). This may or may not have been the actual thickness of the insulation and since it was nearly impossible to monitor the thickness, the nominal value was used. It is believed that the true thickness could have been as low as 21.6 cm (8.5 in.) because of the compression resulting from the weight of the insulation.

Periods in which the model predictions and the data deviated more than expected in Figs. 6 and 7 could be explained by the fact that some of the weather parameters (i.e. wind speed and cloud cover data) used to drive the model were not collected at the exact location of the experimental set up. These data were retrieved from the database of a local airport located approximately 24 km (15 miles) from the test site. A second explanation could be the moisture transport analyses. These were performed using data from relative humidity sensors. When traces of rain were detected, the sensors became saturated and for some period thereafter they recorded erroneous readings. Also, after rainy days, indoor room and attic relative humidities and wood moisture content varied significantly. In the model the wood moisture content was a fixed constant.

A summary of the experimental results using the three values of insulation is presented in Fig. 8. This figure shows average integrated daily ceiling heat flow reduction as a function of insulation level. It is clear that the lower the

amount of insulation, the larger the percent reduction produced by the radiant barrier. One possible explanation is that, with increased insulation level, the surface temperature of the radiant barrier, as well as other parts of the attic, increases. This causes the radiation exchange to occur at higher temperatures, thus, making the relative heat flow reduction smaller.

Although the use of the HRB installation is not widely encouraged for residential applications, the concern about the lower performance because of dust accumulation could be minimized if radiant barrier with low emissivity on both sides is available. A comparison of experimental data on the performance of both the TRB and HRB configurations is presented in Fig. 9. Both configurations showed similar profiles and almost identical heat flux reductions. It was concluded that the HRB slightly outperformed the TRB because the end-gables were not covered in the TRB case. However, it is believed that the differences were within instrument error. While the reductions in heat flux were nearly identical, the TRB showed a significant reduction in attic air temperature when compared to the attic air temperature of the HRB. The temperatures of the shingles were nearly identical in both cases.

Because the outcome of the results was strongly influenced by the indoor temperatures of the houses, in all experiments care was exercised to keep the temperatures inside each house as constant as possible. For the experimental periods presented in this paper, the average difference in indoor temperature between the houses did not surpass 0.2°C (0.3°F).
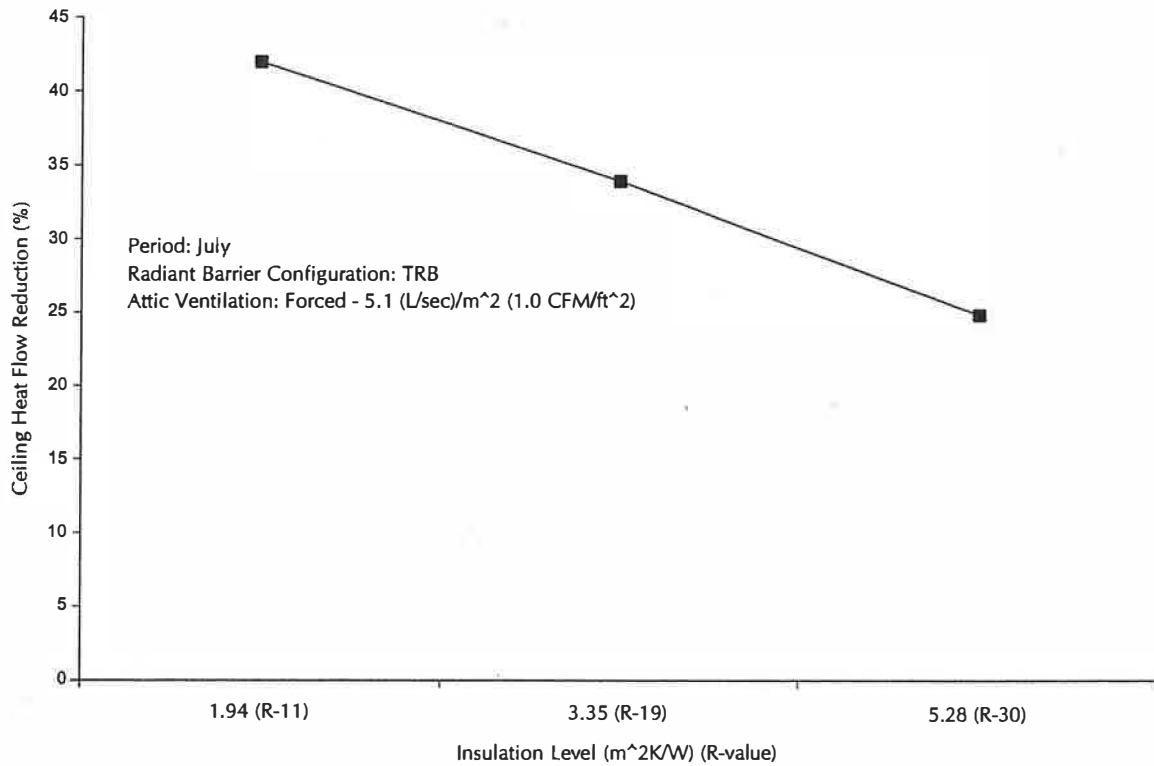
Fig. 8. Heat flow reduction as a function of attic insulation level (experimental).
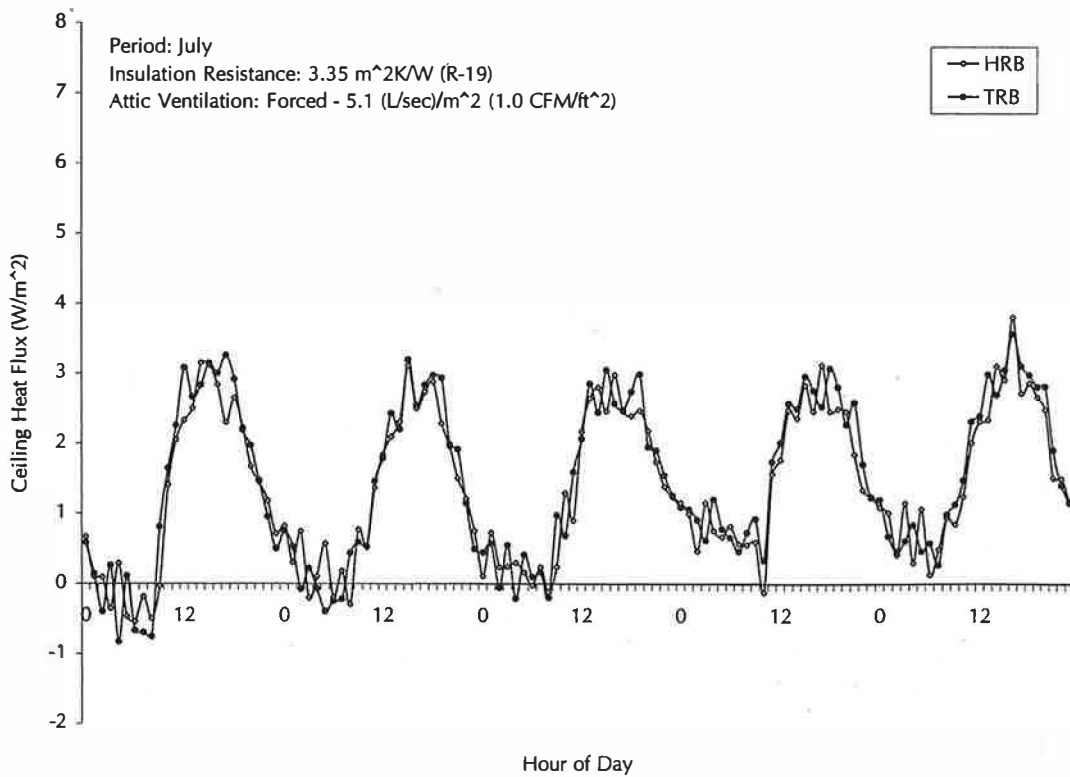

Fig. 9. Comparison between HRB and TRB configurations — experimental (insulation resistance: 3.35 m^2 K/W, R-19; with airflow rate: 5.1 l/s/m^2, 1.0 CFM/ft^2).
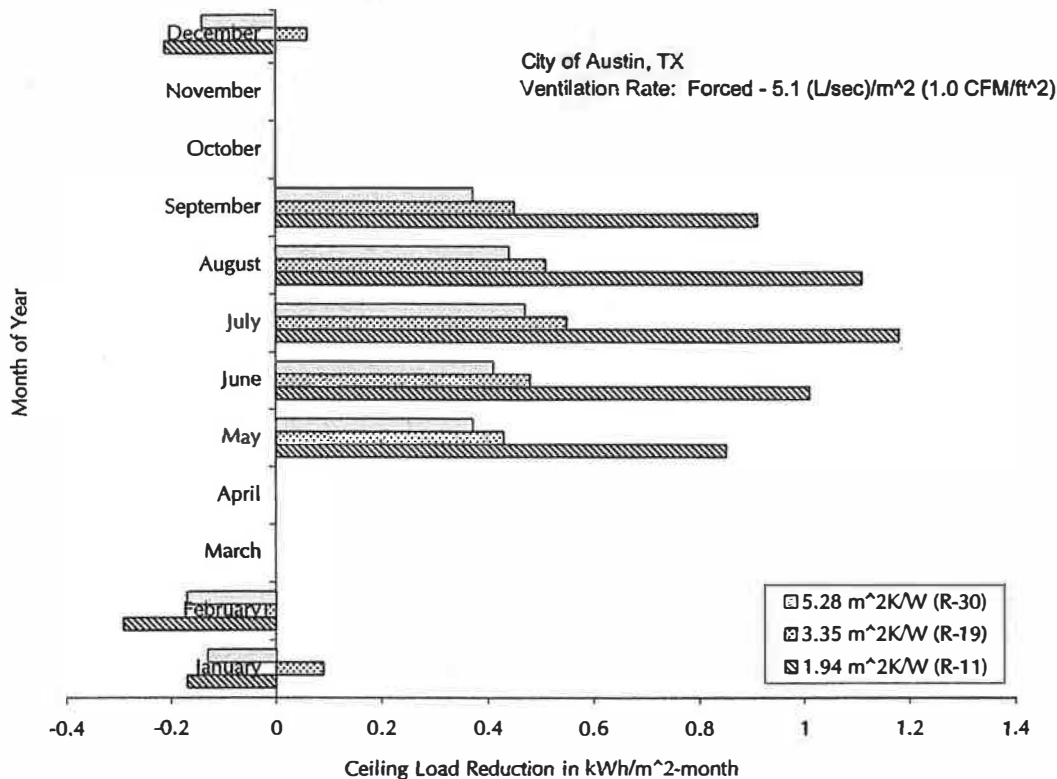
Fig. 10. Monthly ceiling load reductions produced by a TRB under various insulation levels (attic airflow rate: 5.1 l/s/m^2, 1.0 CFM/ft^2).

5. Simulations of monthly performance

The computer model was used to predict the monthly performance of radiant barriers under various ceiling insulation resistances. The weather data used to drive the simulations were from typical meteorological year (TMY) tapes for the City of Austin, TX. Austin weather is categorized as subtropical with hot summers and mild winters. Thirty year climatic averages for Austin indicate high and low summer temperatures of approximately 34°C (94°F) and 23°C (73°F), respectively [13]. The same reference reports summer average percent of possible sunshine for the 30-year average as 73. Reported average winter high and low temperatures were 16.4°C (61.4°F) and 4.8°C (40.6°F), respectively.

Fig. 10 summarizes the amount of ceiling heat load reductions for each kind of insulation level in reference to its corresponding no-RB-case. It is clear from Fig. 10 that reductions in heat flow differ depending on the level of insulation. There are more relative savings under the low insulation case than in the heavily insulated case.

The radiant barrier in combination with insulation with a resistance value of 1.94 m^2 K/W ($R=11$) produced the highest percent reduction compared to an attic without a radiant barrier, 44% on average for yearly aggregates excluding the swing season months of March, April, October and November. In this region, little cooling and/or heating are done during these months.

Reductions in ceiling heat flows, in the range of 28–23%, were realized by the use of radiant barriers in combination with insulation levels of 3.35 m^2 K/W ($R=19$) and 5.28 m^2 K/W ($R=30$), respectively. The model predicted losses in the heating season for two levels of insulation (1.94 and 5.28 m^2 K/W, $R=11$ and 30). It is not known why the middle level of insulation used did not follow the same pattern as the other two in this regard. One of the reasons for predicting these losses is weather related. In Austin, winters are mild with significant sunshine. In monthly simulations in subtropical regions, the savings would either be low (next to insignificant), or negative. Sunshine is a desired feature during the heating season because it reduces the load on heating equipment. Radiant barriers, on the other hand, would limit the amount of solar radiation, which is carried to the conditioned space through the attic. This blockage of infrared radiation from the attic deck is undesirable during the winter season and is the cause of negative savings produced by the radiant barriers. In other regions, this may not be the case and savings could be realized.

6. Conclusions

Experimental as well as simulated results of ceiling heat flow reductions produced by radiant barriers were presented for a subtropical weather pattern. The experimental data resulted from well-controlled experiments using a side-by-

side approach with both houses having identical thermal performance prior to the retrofits. Simulated results were derived from a transient heat and mass transfer model that accurately predicted the reductions in ceiling heat flows in pre-retrofit as well as in retrofit cases for both HRB and TRB configurations. The model captured the relevant thermal and mass processes that take place in buildings.

Percentage reductions in ceiling heat flows, produced by the radiant barriers, were inversely proportional to the level of insulation in the attics. Experimental results during the summer indicated the reductions in ceiling heat flow as 42, 34, 25% for insulation levels of 1.94, 3.35, and 5.28 m^2 K/W (R=11, 19, and 30), respectively. It was also shown that for an insulation level of 3.35 m^2 K/W (R=19) the performances of both the TRB and HRB were nearly identical. Yearly simulations yielded reductions in the range of 44, 28, and 23 for the same levels of insulation, respectively. One possible reason for the discrepancies in savings between the experiments and the simulations could be the number of days used in both cases. During the experiments, the data were produced in 7–10 days while yearly simulations took into account every day in an 8-month period since the 'swing' season months were not used in the simulations. Another reason could be weather related. In the simulated cases, synthesized data from TMY weather files were used. Other reasons, such as the model's ability to capture the mass transfer transports of air and moisture, could be cited.

Acknowledgements

References

[1] J.A. Hall, Performance testing of radiant barriers (RB) with R-11, R-19, and R-30 cellulose and rock wool insulation, in: Proceedings of the Fifth Annual Symposium in Improving Building Energy Efficiency in Hot and Humid Climates, Houston, TX, 1989.

[2] D.G. Ober, T.W. Volckhausen, Radiant barrier insulation performance in full-scale attics with soffit and ridge venting, in: Proceedings of the Fifth Annual Symposium in Improving Building Energy Efficiency in Hot and Humid Climates, Houston, TX, 1989.

[3] W.P. Levins, M.A. Karnitz, D.K. Knight, Cooling energy measurements of unoccupied single-family houses with attics containing radiant barriers, in: Proceedings of the Third Annual Symposium in Improving Building Energy Efficiency in Hot and Humid Climates, Houston, TX, 1986.

[4] M.A. Medina, D.L. O'Neal, W.D. Turner, Effect of attic ventilation on the performance of radiant barriers, ASME J. Solar Energy Eng. 114 (1992) 234–239.

[5] M.A. Medina, D.L. O'Neal, W.D. Turner, A transient heat and mass transfer model of residential attics used to simulate radiant barrier retrofits. Part I. Development, ASME J. Solar Energy Eng. 120 (1998) 32–38.

[6] M.A. Medina, D.L. O'Neal, W.D. Turner, A transient heat and mass transfer model of residential attics used to simulate radiant barrier retrofits. Part II. Validation and simulations, ASME J. Solar Energy Eng. 120 (1998) 39–44.

[7] ASHRAE, Handbook of Fundamentals, American Society of Heating, Refrigeration, and Air Conditioning Engineers, Atlanta, GA, 1989.

[8] B.A. Peavy, A model for predicting the thermal performance of ventilated attics, Summer Attic and Whole House Ventilation, NBS SP 548. Washington, DC, 1979.

[9] E.M. Sparrow, R.D. Cess, Radiation Heat Transfer, Brooks/Cole Publishing Company, Belmont, CA, 1970.

[10] J.A. Duffie, W. Beckman, Solar Thermal Processes, Wiley, New York, 1974.

[11] D.M. Burch, M.R. Lemay, B.J. Rian, E.J. Parker, Experimental validation of an attic condensation model, ASHRAE Trans. 20 (2A) (1984) 59–77.

[12] P.G. Cleary, Moisture control by attic ventilation — an in situ study, ASHRAE Trans. 91 (1) (1985) 227–239.

[13] National Climate Data Center, Asheville, NC, 1999.